

# Multi-epoch Spectroscopy of IY UMa: Quiescence, Rise, Normal Outburst & Superoutburst

Daniel J. Rolfe<sup>1,2</sup>, Carole A. Haswell<sup>1</sup>, Timothy M. C. Abbott<sup>3,4</sup>

Luisa Morales-Rueda<sup>5,6</sup>, T. R. Marsh<sup>5,7</sup> and G. Holdaway<sup>5,8</sup>

<sup>1</sup>*Department of Physics & Astronomy, The Open University, Walton Hall, Milton Keynes, MK7 6AA, UK.*

<sup>2</sup>*Department of Physics & Astronomy, University of Leicester, University Road, Leicester, LE1 7RH, UK.*

<sup>3</sup>*Cerro Tololo Inter-American Observatory, Casilla 603, La Serena, Chile*

<sup>4</sup>*Nordic Optical Telescope, Roque del Los Muchachos & Santa Cruz de La Palma, Canary Islands, Spain*

<sup>5</sup>*Department of Physics & Astronomy, Southampton University, Southampton, SO17 1BJ, UK.*

<sup>6</sup>*Department of Astrophysics, University of Nijmegen, P.O. Box 9010, 6500 GL Nijmegen, The Netherlands.*

<sup>7</sup>*Department of Physics, University of Warwick, Coventry, CV4 7AL, UK.*

<sup>8</sup>*Fault Studies & Fuel Branch, British Energy Generation Ltd, Gloucester, GL4 3RS*

Accepted. Received

## ABSTRACT

We exploit rare observations covering the time before and during a normal outburst in the deeply-eclipsing SU UMa system IY UMa to study the dramatic changes in the accretion flow and emission at the onset of outburst. Through Doppler tomography we study the emission distribution, revealing classic accretion flow behaviour in quiescence, with the stream-disc impact ionizing the nearby accretion disc. We observe a delay of hours to a couple of days between the rise in continuum and the rise in the emission lines at the onset of the outburst. From line profiles and Doppler maps during normal and superoutburst we conclude that reprocessing of boundary layer radiation is the dominant emission line mechanism in outburst, and that the normal outburst began in the outer disc. The stream-disc impact feature (the ‘orbital hump’) in the  $H\alpha$  line flux light curve disappears before the onset of the normal outburst, and may be an observable signal heralding an impending outburst.

**Key words:** stars: novae, cataclysmic variables, stars: individual: IY UMa, stars: dwarf novae, techniques: spectroscopic

## 1 INTRODUCTION

IY UMa is an SU UMa type dwarf nova cataclysmic variable (CV). These are systems in which a white dwarf accretes via Roche lobe overflow from the donor, forming an accretion disc around the white dwarf which undergoes a series of short normal outbursts ( $\sim 5$  days for IY UMa), and longer superoutbursts ( $\sim 3$  weeks). The outbursts are thought to result from the switching of the disc between a cool, neutral, low-viscosity state and a hot, ionised viscous state. In the cool state very little mass is transferred inwards, while in the hot state mass is rapidly accreted onto the white dwarf. Superoutbursts are thought to differ from normal outbursts due to the onset of a tidal instability in the disc, in which a 3:1 resonance between tidal forces and orbits of particles in the disc leads to a distorted, precessing disc. Periodic luminosity modulations, called superhumps, with periods a few per cent longer than the orbital period are the defining characteristic of superoutbursts. Superhumps result from the in-

teraction of the donor orbit with the eccentric disc. For a review see Osaki (1996) and for a recent discussion Osaki & Meyer (2003).

Patterson et al. (2000, hereafter P2000) and Rolfe, Haswell & Patterson (2001b) present detailed photometric studies of IY UMa’s January 2000 superoutburst and superhumps. Spectroscopic observations reveal a bright hotspot and deep white dwarf absorption lines during quiescence (Rolfe, Abbott & Haswell 2001a; Patterson et al. 2000); an eccentric disc during superoutburst (Wu et al. 2001); lines powered by reprocessed boundary layer emission during outburst (Rolfe, Abbott & Haswell 2002a) and an M dwarf donor star (Rolfe, Abbott & Haswell 2002b).

We present spectroscopic observations of IY UMa in quiescence, rise, in outburst and in superoutburst. Section 2 presents the observations. In Section 3 we discuss the average spectra epoch by epoch. We cover the lightcurves in Section 4 and the line profile variations and detailed ac-

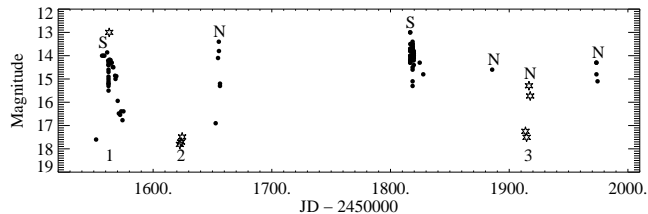


**Figure 1.** VSNET observations of IY UMa outbursts (circles) and observing runs presented in this work (stars). 'S' denotes a superoutburst, 'N' a normal outburst. The observations are marked: 1 - WHT, January 2000, 2 - NOT, March 2000 and 3 - NOT, January 2001.

tion flow in Section 5. In Sections 6 and 7 we discuss and summarise our findings.

## 2 OBSERVATIONS AND DATA REDUCTION

Fig. 1 marks our observations in relation to the longterm lightcurve from the VSNET network.

Orbital phases for all observations in this work were calculated using the white dwarf ephemeris in P2000.

### 2.1 WHT

On 2000 January 19 we used the ISIS double beam spectrograph on the 4.2m William Herschel Telescope (WHT) on La Palma (see Table 1 for details) to monitor  $H\alpha$  and  $He I$  6678Å in the red arm and  $H\gamma$ ,  $H\beta$ ,  $He II$  and several  $He I$  lines in the blue arm.

Standard CCD processing, optimal extraction of spectra (Marsh 1989), wavelength calibration and instrumental response and extinction corrections were performed. Uncertainties on every point were propagated through every stage of the data reduction.

As we did not put a comparison star in the slit with IY UMa the spectra have not been corrected for slit losses. This means that the variability seen from one spectrum to the next could be due to passing clouds and it is most probably not due to the intrinsic variability of the system.

### 2.2 NOT

The Nordic Optical Telescope (NOT) observations comprise about 14 binary orbits of spectra from 2000 March and 2001 January taken using the ALFOSC spectrograph (see Table 1).

The 2000 March observations were reduced and flux calibrated following standard procedures without corrections for slit losses. The March 18th spectra are reliable only between about 4000Å and 5200Å due to wavelength calibration problems.

The 2001 January exposures of IY UMa included a nearby comparison star for correction of slit losses. Wide slit exposures of IY UMa and the comparison, and of a flux standard, were taken and used for flux and slit loss calibration.

The 2001 Jan observations were fully flux calibrated and slit loss corrected above  $\sim 4800$ Å and degraded only by the wavelength dependent slit losses at shorter wavelengths.

**Table 1.** The observations.  $\Delta\lambda$  is the FWHM spectral resolution  $N$  is the number of spectra. The instrument column lists the grating, CCD and readout mode for the red and blue ISIS arms in WHT observations and the grism number for the NOT observations.

Tel. Date	Instr.	Orbits	N	Exp. (s)	$\lambda$ range (Å)	$\Delta\lambda$ (Å)
WHT	ISIS					
19/1/00	R1200R	1.4	64	80	6350–6750	0.8
	Tek/Quick R1200B	1.3	53	80	4270–5070	0.9
	EEV/Std.					
NOT	ALFOSC					
18/3/00	6	4.1	59	300	3180–5550	6
19/3/00	7	2.9	80	180	3820–6840	6
20/3/00	7	1.6	64	120	3820–6840	5
3/1/01	8	1.6	21	360	5810–8350	5
4/1/01	8	1.2	18	360	5810–8350	5
6/1/01	7	1.1	58	60	3820–6840	5
7/1/01	7	2.2	131	60	3820–6840	5

## 3 AVERAGE SPECTRA

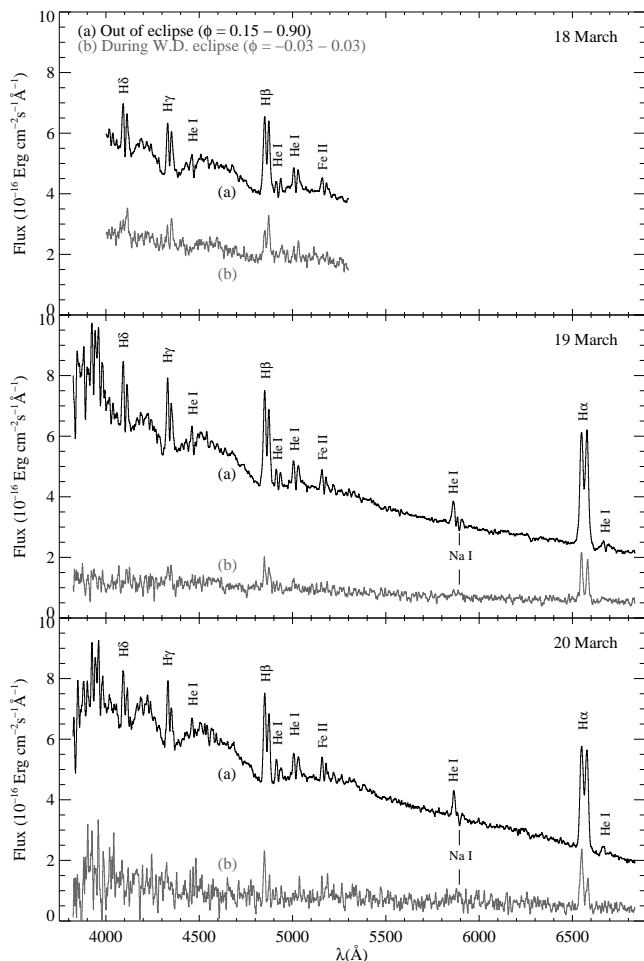
### 3.1 2000 March: IY UMa in quiescence

Fig. 2 shows 2000 March average nightly spectra during and outside eclipses (phase ranges given in Fig. 2). The spectra have been smoothed by slightly less than the instrumental resolution. Strong, double-peaked Balmer,  $He I$  and  $Fe II$  emission lines are superimposed on a blue continuum. Broad absorption wings are seen around the Balmer emission lines except  $H\alpha$  and there are deep cores between the double peaks of the lines, reaching below the continuum in some cases. Such features are seen in two other high inclination dwarf novae in quiescence - Z Cha (Marsh, Horne & Shipman 1987) and OY Car (Hessman et al. 1989). Weak NaI doublet absorption at 5890–5896Å is superimposed on  $He I$  5876Å.

The full width of the Balmer absorption wings is about  $20,000 \text{ km s}^{-1}$ , far too large to be Doppler-shifted disc material. The broad absorption wings disappear during the white dwarf eclipse; we conclude that these features come predominantly from the white dwarf (c.f. Marsh et al. 1987). The absorption cores remain during the white dwarf eclipse, indicating they arise at least partially in the disc.

#### 3.1.1 The hotspot spectrum

The very high inclination of IY UMa (c.f. Steeghs et al. 2003) leads to a prominent orbital hump as the hotspot comes into view. The hotspot spectra in Fig. 3 were produced by subtracting the average spectrum around hump minimum (orbital phases 0.5 to 0.6) from that around hump maximum (phases 0.75 to 0.9). Strong emission lines in the Balmer series and weaker emission in  $He I$  and  $Fe II$  are superimposed on a blue continuum. The lines show one strong peak indicating a concentrated emission region, with some weaker peaks and dips arising from changes in line profile between the hump maximum and minimum.



**Figure 2.** Average spectra of IY UMa during quiescence in March 2000.

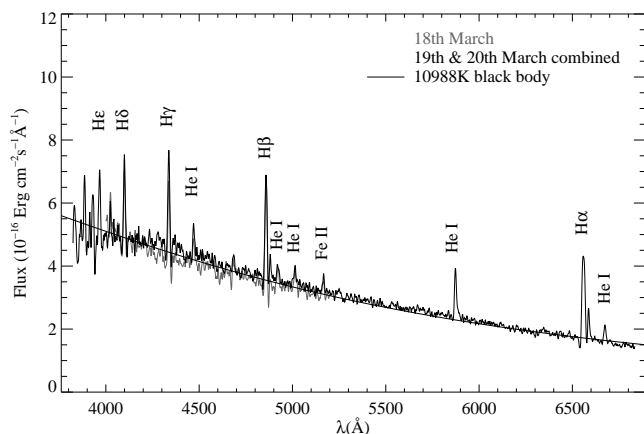


**Figure 3.** The spectrum of the orbital hump, obtained by subtracting the average spectrum at hump minimum from the average at hump maximum (smoothed as in Fig. 2). The smooth curve is the blackbody fit.

Fig 3 shows a simple blackbody spectrum fit (assuming  $d = 190 \pm 60$  pc, from P2000) which has a temperature  $T = 10990 \pm 120$  K and emitting area  $A = 3.8^{+3.0}_{-2.1} \times 10^{18} \text{ cm}^2$  ( $= 0.0015^{+0.0011}_{-0.0008} a^2$  where  $a$  is the orbital separation). The emission lines were masked out. The error in  $T$  is a 90 per cent confidence estimate where the confidence region was determined using a Monte-Carlo “bootstrap”-type resampling and fitting of the data 30000 times. The error in  $A$  is dominated by propagating the uncertainty in  $d$ . Systematic errors are not accounted for in these confidence limits, e.g. errors in the atmospheric extinction correction and any deviation of the real spectrum from the assumed blackbody form. The latter is hard to detect since we only sample the tail of the Rayleigh-Jeans distribution. Marsh et al. (1987) produced a hotspot spectrum for Z Cha using the same technique, finding a non-blackbody continuum, with a significant drop below  $4000 \text{ Å}$ , probably due to Balmer absorption. The effective area determined here is consistent with the simple stream-disc impact model used for IY UMa in Rolfe et al. (2001b). The temperature is typical: hotspot temperatures of  $\sim 10000$ – $20000$  K were found by Stanishev et al. (2001); Robinson et al. (1995); Wood et al. (1986).

### 3.2 2001 January: IY UMa rises to normal outburst

Fig. 4 shows the average spectra; for 2001 Jan 3 and 4 we show just the blue end of the red spectra which were discussed in Rolfe et al. (2002b). The phase ranges used are given in Fig. 4. On 2001 Jan 3 and 4 the system is quiescent, the only notable difference from 2000 March being the deeper core between the disc peaks.

On 2001 Jan 6 the system is 7-8 times brighter. Deep core absorption is seen in all emission lines except  $H\alpha$ . This resembles OY Car during a normal outburst (Harlaftis & Marsh 1996) and some superoutburst spectra of Z Cha (Honey et al. 1988). The Balmer absorption wings are no longer seen, meaning that the deep core absorption in outburst cannot be due to the white dwarf. This also adds weight to the suggestion that the cores in quiescence are not entirely due to the white dwarf absorption. The  $4640 \text{ Å}$  C III/N III Bowen blend and He II  $4686 \text{ Å}$  have appeared, as in IY UMa in superoutburst (Wu et al. 2001), in other dwarf novae in outburst (Morales-Rueda & Marsh 2002) and in nova-likes e.g. V348 Pup and UX UMa (Tuohy et al. 1990; Rolfe 2001; Rutten et al. 1993). The He II emission probably results from the reprocessing of EUV and X-ray boundary layer emission (Patterson & Raymond 1985), while the N III emission may come from conversion of He II Ly $\alpha$  transition photons to N III photons via O III (Deguchi 1985).

On 2001 Jan 7 the continuum is about 30 per cent less than Jan 6 and the line absorption cores are much weaker. He II  $4686 \text{ Å}$  and the Bowen blend are much stronger, with He II comparable in strength to  $H\beta$ . He II  $5412 \text{ Å}$  is faintly visible. The He II  $4686 \text{ Å}$  line profile is consistent with strong double-peaked emission from the disc blended with a C III/N III and He I  $4713 \text{ Å}$  contribution. The most obvious absorption feature is He I  $4471 \text{ Å}$ . This has low velocity, is very narrow, and disappears almost precisely during the WD eclipses (Fig. 4), implying absorption occurring close to the WD.

IY UMa went into outburst between Jan 4 and Jan 6,





7 (2001 Jan). “Continuum B” is the flux integrated in the range 4000Å–5200Å (covered by all the March 2000 spectra) while “Continuum R” is over the range 5950Å–6450Å (covered by all the 2000 and 2001 spectra except 2000 March 18). For  $H\beta$ , the average flux either side of the profile was subtracted to reduce the effect of the absorption wings. Note that slit loss corrections were not possible for the 2000 March observations, but the data suggest that apart from the omitted phase range 2–2.5 on 18 March, conditions were photometric. The 2000 January observations conditions were not photometric and no slit loss correction was possible, so we do not present lightcurves for these data.

#### 4.1 2000 March: quiescence

The continuum lightcurves for 2000 March reveal the strong orbital hump and eclipse seen in photometry (P2000, Rolfe et al. 2001b). On 2000 March 19 and 20 there is a double-humped structure, with the usual strong orbital hump peaking around phase 0.8–0.9 and a weaker hump peaking around 0.3–0.4. The strong hump is the stream-disc impact coming into view on the near side of the disc while the weak hump is when the stream-disc impact is again seen roughly length ways, but on the far side of the disc. Similar orbital curves have been seen in WZ Sge and AL Com (Robinson, Nather & Patterson 1978; Patterson et al. 1996), but with both humps having the same amplitude.  $H\alpha$  and  $H\beta$  show a stronger secondary hump and a shallower eclipse, the latter resulting from disappearance of the unsubtracted core of the white dwarf Balmer absorption lines during eclipse (an effect which is stronger for  $H\beta$ ).

#### 4.2 2001 January: normal outburst

The Jan 3 and 4 continuum curves (Fig. 7) show a single orbital hump; the flux away from hump and eclipse is within a factor  $\sim 2$  of March 2000. The hump is about twice as bright on Jan 3 as on Jan 4. The  $H\alpha$  curves on Jan 4 shows no sign of the hump. Though low time resolution and phase coverage prevents detailed analysis, we see changes in the behaviour of the system over one day. If it is linked to the following outburst, this is important. No advanced warning of an impending outburst has been seen before.

Between Jan 4 and 6, the continuum flux rises by a factor of  $\sim 7$ , decreasing again by the beginning of the Jan 7’s observations. During Jan 7 the flux drops by a further 20 percent. The eclipses are all deep, with the eclipse during orbit 42 broader and shallower than those during orbits 55 and 56. This implies the light distribution becomes more concentrated around the white dwarf between Jan 6 and 7; suggesting the outer disc is returning to quiescence. Measurement by eye yields full eclipse widths which correspond to emission distributions of radius  $0.37 \pm 0.10a$  on Jan 6 shrinking to  $0.21 \pm 0.05a$  on Jan 7. These radii are both much smaller than the 3:1 resonance radius ( $0.46a$ ) indicating a normal outburst. n.b. P2000 measured radius  $0.44 \pm 0.03a$  in super-outburst. An unrealistic eccentricity ( $\sim 0.8$ ) is needed for a non-circular disc to explain the change in eclipse width.

The eclipses are fairly symmetrical, and centred on phase 0, suggesting emission centred on the white dwarf. In contrast with the continuum, the emission lines all rise

on Jan 6, being nearly twice as bright at the start of the observations on Jan 7 than during Jan 6. These changes are not simply a result of variations in the core absorption. The delay in rise of the lines relative to the continuum is between about one orbit and two days. On the 2001 Jan 7 the EWs in  $H\alpha$  and  $He II$  increase by about 7–8 per cent. The  $H\alpha$  eclipses suggest the same decrease in radius of the line emission region as for the continuum. The  $H\alpha$  EW doubles during eclipse, while for  $He II$  it decreases almost to zero. We conclude the  $He II$  emission comes from a smaller area than  $H\alpha$ , concentrated closer to the white dwarf.

### 5 DOPPLER TOMOGRAPHY

Doppler tomography (Marsh & Horne 1988) exploits phase-resolved emission line profiles to produce velocity-space maps of the emission distribution. It assumes the emitting material and its velocities are in the orbital plane, that the brightness and visibility of each point do not vary with phase, and that the intrinsic line profile is narrow compared with the Doppler shifts due to the velocity distribution. We excluded data from phases  $-0.1$  to  $0.1$  since eclipses occur then. The hotspot also has a varying brightness, so Doppler maps indicate only an orbital average of the hotspot emission. The Fourier-filtered back projection technique was used to produce the maps. Levels below the continuum are shown the same as the continuum level.

#### 5.1 2000 March: quiescence

The trailed spectra in 2000 March revealed the same orbital modulation throughout. We therefore consider the phase-folded trails shown in the top row of Fig. 8. Double-peaked emission with eclipse first in the blue peak and then in the red, as expected from a prograde disc, is seen in the Balmer lines. The disc emission in the red wing around phase 0.3 is weaker than at other phases (except eclipse), with this being very clear in  $H\gamma$ . A similar effect was seen in WZ Sge by Spruit & Rutten (1998), where an S-wave of absorption was seen delayed in phase relative to the hotspot S-wave. The brightening in the blue wing around phase 0.3 is a distinct feature, not simply the coincidence of the stream and disc emission. This could result from a bright region of the disc on the opposite side from the donor. Between the disc peaks is the core and white dwarf Balmer absorption. A strong S-wave with phase-dependent brightness and the same phasing and amplitude appears in all four lines. The strength of the disc emission is similar to that of the S-wave emission in  $H\alpha$ , but the relative strength of disc to S-wave decreases for higher order Balmer lines, with the brightest parts of the S-wave dominating in  $H\gamma$ . The bottom panel of Fig. 8 shows the trails after subtracting the average line profile in the phase range 0.1–0.9. This removes much of the disc profile and core absorption, revealing that S-wave brightness follows that of the orbital hump (c.f. Fig. 6). The S-wave is eclipsed late indicating an origin at the stream-disc impact. The sharp brightening in the S-wave/red wing around phase 0.2 results from poor phase coverage around phase 0.20–0.25 on 19 and 20 March.

The four Doppler maps (Fig. 8, Row 2) show absorption at low velocity corresponding to the deep cores vis-

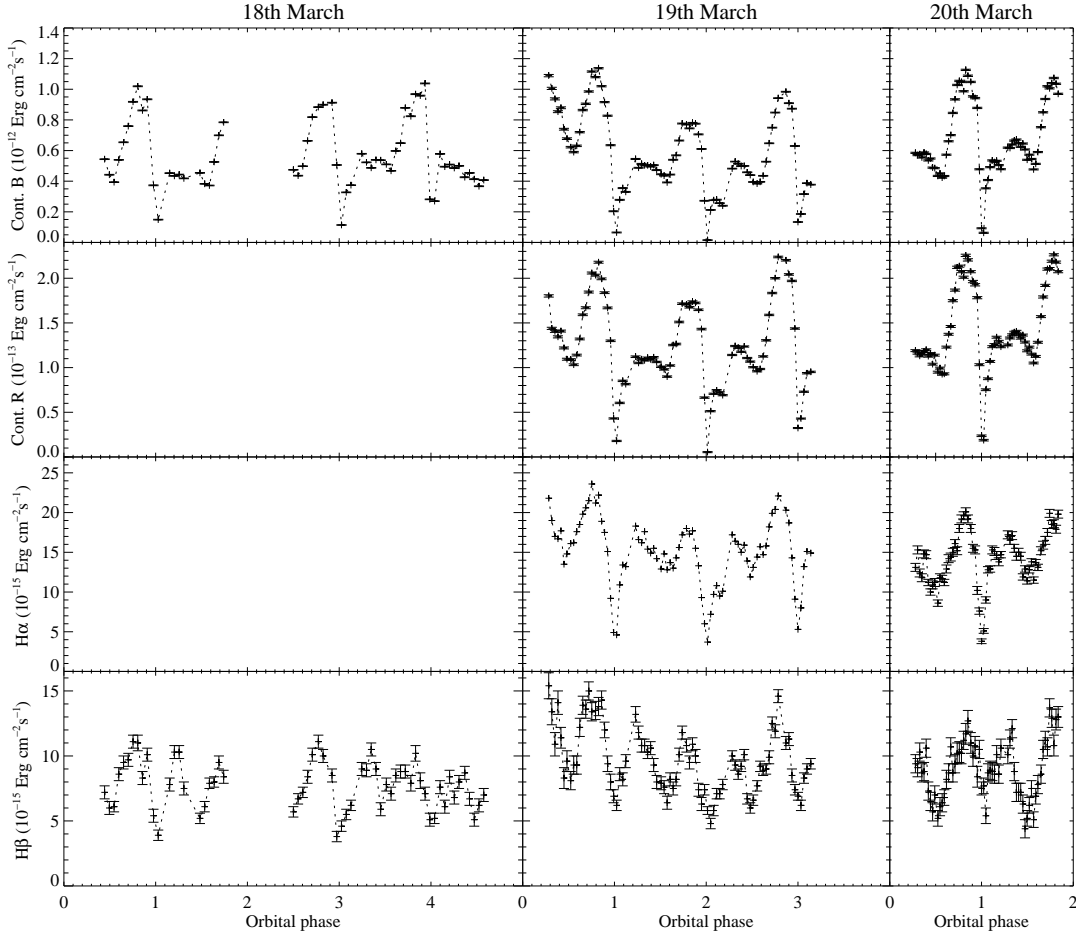


**Figure 6.** March 2000 quiescence average orbital lightcurves

ible in the average spectra. The  $H\alpha$  map shows emission from disc material within the tidal radius. The stream-disc impact is seen between the two arcs corresponding to the stream trajectory and its Keplerian velocity (c.f. U Gem, Marsh et al. (1990) and WZ Sge, Spruit & Rutten (1998)). This is also seen in SPH simulations where more detail is apparent (Foulkes et al. 2004). The  $H\alpha$  disc emission is weaker where the two arcs cross it. Spruit & Rutten (1998) point out that the stream-disc impact is hot enough to ionize hydrogen, suppressing Balmer emission until further downstream where the hydrogen has recombined. If the hydrogen in the converging stream and disc flows is ionized, then we expect the Balmer emission from this region to be suppressed. The light curves of Steeghs et al. (2003) suggest that IY UMa's extreme edge-on inclination affords us a view into a hot shock-heated cavity driven into the disc by the stream impact. SPH simulations (Foulkes et al. 2004) suggest that the dissipation at the impact occurs in both the stream and the disc flows, and is localised at the impact velocity of each. The March 2000  $H\alpha$  map is suggestive of ionisation caused in this way. The  $\sim 11000$  K blackbody hotspot temperature found in IY UMa (c.f. Fig. 3) would be sufficient to ionize hydrogen.

The third row of Fig. 8 shows the line profiles reconstructed from the Doppler maps i.e. the line profiles we would see if the emission distribution was exactly as shown

in the Doppler map, and all assumptions of Doppler tomography were valid. Comparing the reconstructed trails with the observed ones provides a useful measure of how reliable the Doppler maps are. Eclipses (not accounted for in Doppler tomography) are omitted, but we see clearly in the reconstructed trails the same disc and hotspot features as in the observations, but with features resulting from intrinsic variations during the orbit (the hotspot orbital hump) not correctly reproduced, since the Doppler map is an orbital average. The Doppler map has attempted to reproduce the orbital hump by superposing sine waves of differing velocity amplitude. This leads to the emission extending out to  $\sim 2000 \text{ km s}^{-1}$  at orbital phase 0.5, for which there is no evidence in the observed trails.

## 5.2 2001 January: normal outburst

In Jan 2001 we observed the accretion flow behaviour around the rise from quiescence to normal outburst.

### 5.2.1 2001 Jan 3,4: pre-rise

Trailed spectra from 2001 Jan 3 and 4 for  $H\alpha$ , and He I  $5876\text{\AA}$  are shown in Fig. 9. The wavelength of the weak Na I absorption doublet line at  $5890\text{--}5896\text{\AA}$  corresponds to a velocity range of about  $700\text{--}1000 \text{ km s}^{-1}$  relative to He I

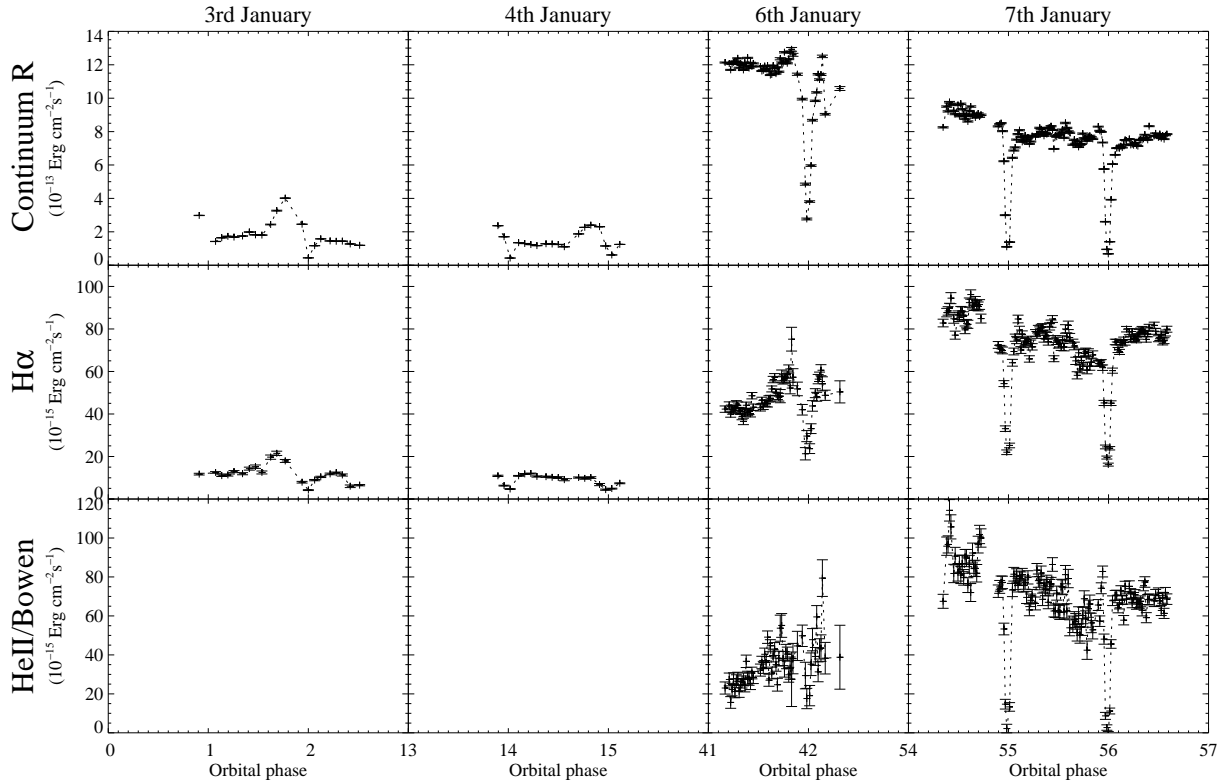


Figure 7. Jan 2001 lightcurves during quiescence, rise, and normal outburst.

5876Å so we must be wary of this when studying this line. H $\alpha$  shows double peaks and a blue-to-red eclipse; the S-wave is not visible, although brighter regions in the peaks hint at its presence, particularly on 2001 Jan 4. The low S/N in He I prevents any structure being seen in that trail, apart from the core/Na I absorption and possibly a bright region around the blue peak between about phase 0.6 and 0.75, maybe due to an S-wave.

Doppler maps for 2001 Jan 3 and 4 (Fig. 9) are blurred by  $\sim 20^\circ$  by the long exposures and the limited number of spectra. Despite this all 4 maps show evidence of the hotspot at the same location as in 2000 March, with He I a little further upstream than the H $\alpha$  hotspot.

### 5.2.2 2001 Jan 6: outburst

The 2001 Jan 6 H $\alpha$ , H $\beta$ , H $\gamma$  and He I 5016Å trails (Fig. 10) all show double-peaked disc emission, while the blue-to-red eclipse is seen clearly in H $\alpha$  and H $\beta$  (the strongest lines). Apart from the rise in brightness throughout the night, there is no other easily identifiable behaviour. Deep absorption cores hide any structure between the peaks.

The 2001 Jan 6 Doppler maps (Fig. 10, 2nd row) differ considerably from those for 2001 Jan 3 and 4. The H $\alpha$  map shows a ring of disc emission which has two bright regions on opposite sides of the disc around maximum and minimum  $V_y$ . The same structure is seen in H $\beta$  and H $\gamma$ . The He I map is noisier but consistent. The two-fold asymmetry is an artefact from leaving out the eclipse phases: omitting the disc emission during eclipse weakens the left and right sides of the ring in the map, while missing the very strong core ab-

sorption during eclipse enhances the strip around  $V_x = 0$  in the map, accentuating the top and bottom of the disc ring. The brightening of the line flux during the night (c.f. Fig. 7) biases the map, and may thus contribute to the two-fold asymmetry. We therefore made a set of maps (Rolfe, 2001) using spectra normalised so the total line flux remained constant with time. H $\alpha$  showed similar asymmetries to those of the maps in Fig. 10 while the other lines produced inferior maps due to the effects of noise in the integrated line flux. Accordingly we conclude the maps from 2001 Jan 6 show no more than emission from a disc within the tidal radius.

Each map for 2001 Jan 6 had its azimuthally averaged map subtracted (Fig. 10, third row), enhancing non-axisymmetric features. This removes much of the disc ring and the central absorption. The Balmer maps clearly show emission coming from the velocity of the donor star. The quality of the He I map is too poor to identify or rule out such a feature. The reconstructed trails show clearly the disc emission and core absorption, with the double peaks disappearing around phase 0.5 in contradiction with the observations, confirming the conclusion that the asymmetry in the Doppler maps is an artefact of omitting eclipses.

We subtracted the average line profiles for the phase range 0.2–0.8 from the observed trails (Fig. 10, bottom row), reducing the disc and absorption components. Overplotted is the expected velocity of the donor star. There is clear evidence of a weak emission component in H $\alpha$  following the donor velocity. This confirms that there is emission from the donor velocity, and that this is not merely an artefact in the Doppler maps, at least in the case of H $\alpha$ .

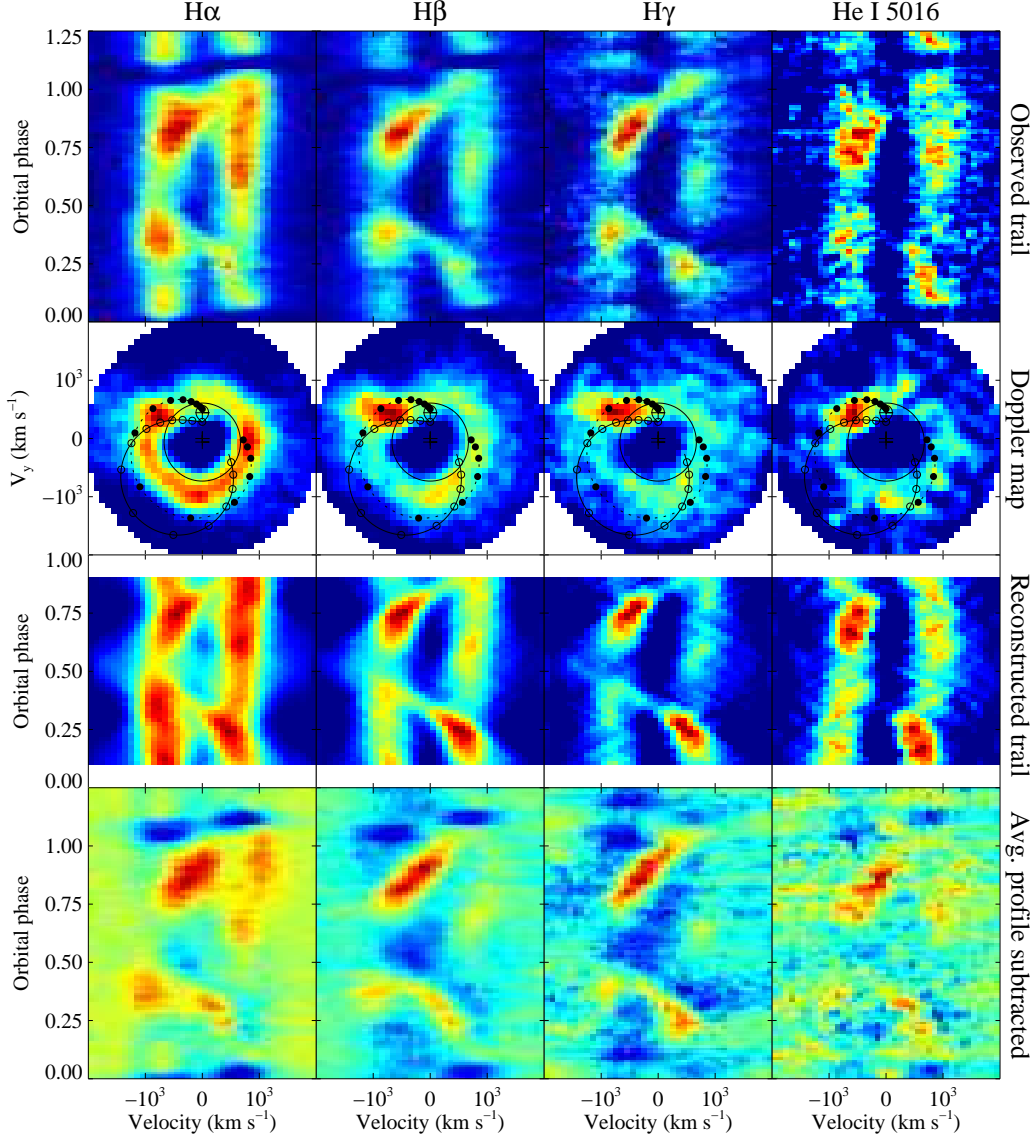


**Figure 8.** Doppler tomography combining all 3 nights of data during quiescence in March 2000. *Top row:* Phase-folded, phase-binned, velocity-binned and continuum-subtracted trailed spectra. Phases 0–0.25 are repeated. *Second row:* Fourier-filtered back-projections. Emission from the donor star should appear within the black teardrop. Disc emission should appear outside the black circle (the Keplerian velocity at the radius where the disc is tidally truncated). The ballistic stream velocity is the arc with unfilled circles, and the arc with filled circles is the Keplerian velocity along the stream trajectory. These markings assume the orbital parameters of P2000. *Third row:* Trailed spectra reconstructed from Doppler maps. *Bottom row:* Observed trail minus average line profile in phase range 0.1 to 0.9.

### 5.2.3 2001 Jan 7: Decline

The Balmer trails (Fig. 11) reveal more complicated structure than on 2001 Jan 6 because the absorption cores are substantially weaker. The behaviour is stable throughout the night and is the same for all four lines, except that the core is deeper for higher-order lines. There are double peaks and the clear blue-to-red eclipse. There is a clear S-wave with velocity semi-amplitude  $\sim 300\text{--}600\text{ km s}^{-1}$ , maximum redshift around phase 0.25, disappearing from about phase -0.2 to 0.2. This S-wave appears to originate on the inner face of the donor star. The velocity, phasing and invisibil-

ity at phase -0.2 to 0.2 all suggest this, c.f. IP Peg during outburst e.g. Morales-Rueda, Marsh & Billington (2000).

The trails suggest another S-wave. In the blue disc wing around phase 0.4 centred on a velocity of about  $-700\text{ km s}^{-1}$ , we see a bright region which covers a phase range of less than 0.1, and a velocity range of more than  $500\text{ km s}^{-1}$ . This is seen in all three orbits in H $\alpha$  and H $\beta$ , and can also be seen more faintly in H $\gamma$  and He I. In the first orbit in the red wing at phase 0.9 we see a similar feature at velocity of about  $700\text{ km s}^{-1}$ , probably the opposite extremum of the same S-wave, but much fainter, c.f. OY Car (Harlaftis & Marsh 1996).



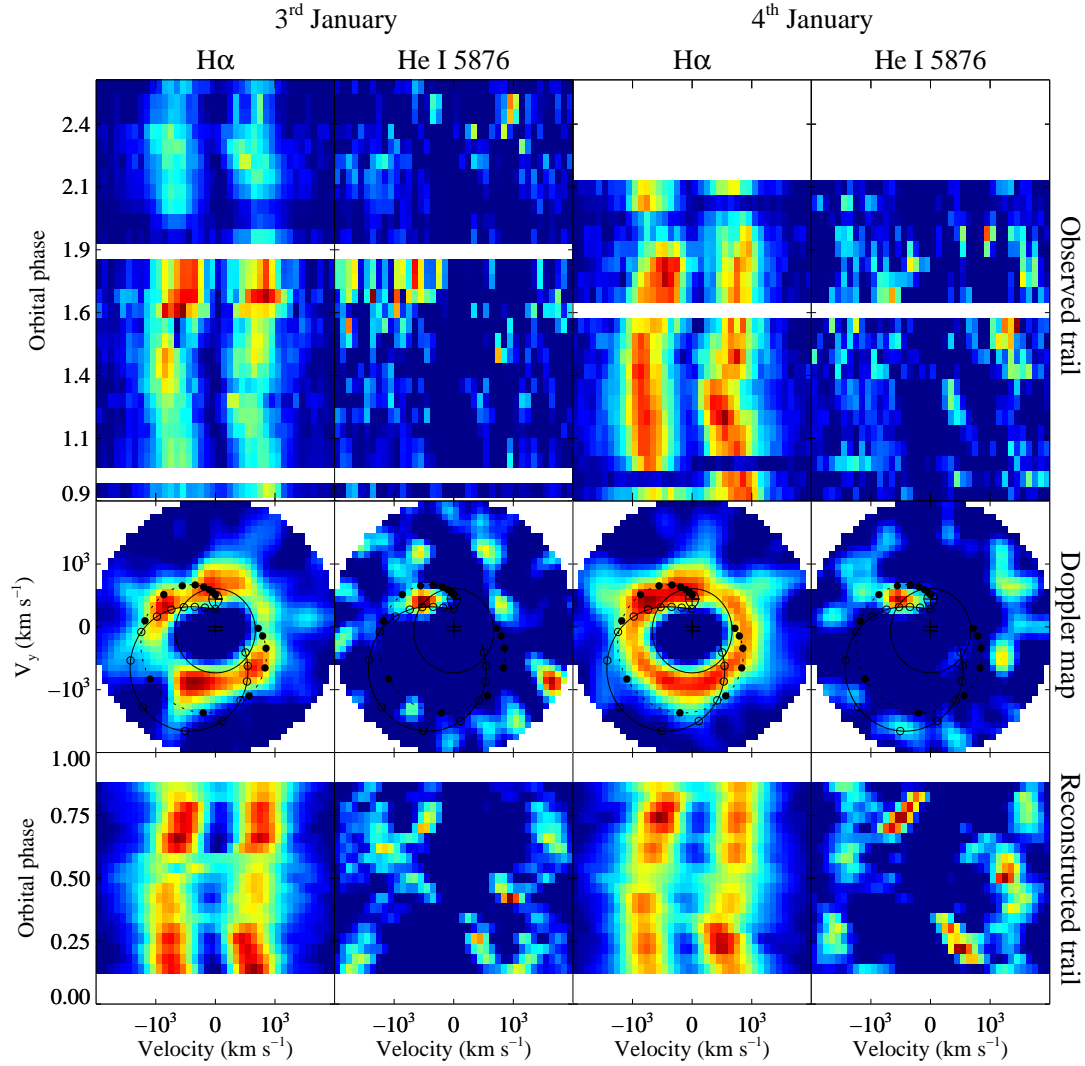


**Figure 9.** Doppler tomography before outburst in Jan 2001. *Top row:* Phase-binned, velocity-binned and continuum-subtracted trailed spectra. *Other rows:* As in Fig. 8.

The middle row of Fig. 11 shows the Doppler maps for Jan 7. The Balmer and He I 5016Å maps show strong emission concentrated around the velocity of the donor star, confirming our inference from the trails and less directly from the maps from the previous night. Given the resolution, this source is consistent with emission from the inner face of the donor. Emission from the donor star during outburst has been seen before, e.g. OY Car (Harlaftis & Marsh 1996) and IP Peg (Steehls 2001; Morales-Rueda et al. 2000; Marsh & Horne 1990). Irradiation-driven He II 4686Å emission was present in these systems, as in IY UMa (Fig. 11). Marsh & Horne (1990) and Harlaftis & Marsh (1996) concluded that EUV emission and X-ray emission from the boundary layer (BL) could drive the Balmer emission. The Balmer emission in IY UMa is correlated with He II (Fig. 7), suggesting the same driving mechanism.

The other notable feature seen in the Jan 7 maps is an arc of emission on the left hand side (negative  $V_x$ ) at velocities corresponding to the outer part of the disc. We do not see the full circle corresponding to the whole disc. The arcs are brightest around  $V_y = 0$ . In Hα and Hβ the

arc stretches through about 270° (measured anti-clockwise from the donor velocity), while in Hγ and He I it only reaches about 135°, although He I shows a bright blob around 225°. This structure appears similar to that seen in outburst in OY Car by Harlaftis & Marsh (1996), which followed and was thus attributed to the accretion stream. However, in IY UMa this is not the case; it follows the velocity of the outer disc and no stream-disc impact hotspot is seen, so this emission does not arise from dissipation of energy where the stream hits the disc edge. Despite the lack of emission from dissipation of kinetic energy at the stream-disc impact, some vertically extended structure is likely to be present where the stream impacts the disc, providing a region where we might see reprocessing of the EUV and X-rays from the BL, simply because vertically extended structure will intercept more BL radiation. This would be top left in the Doppler maps. If this vertical structure, raised at this point initially by the stream disc impact, extended further around the disc, it could explain the brightest region of the emission line arcs seen here. The inner face of this raised region should appear bright, being directly irradiated, explaining why the

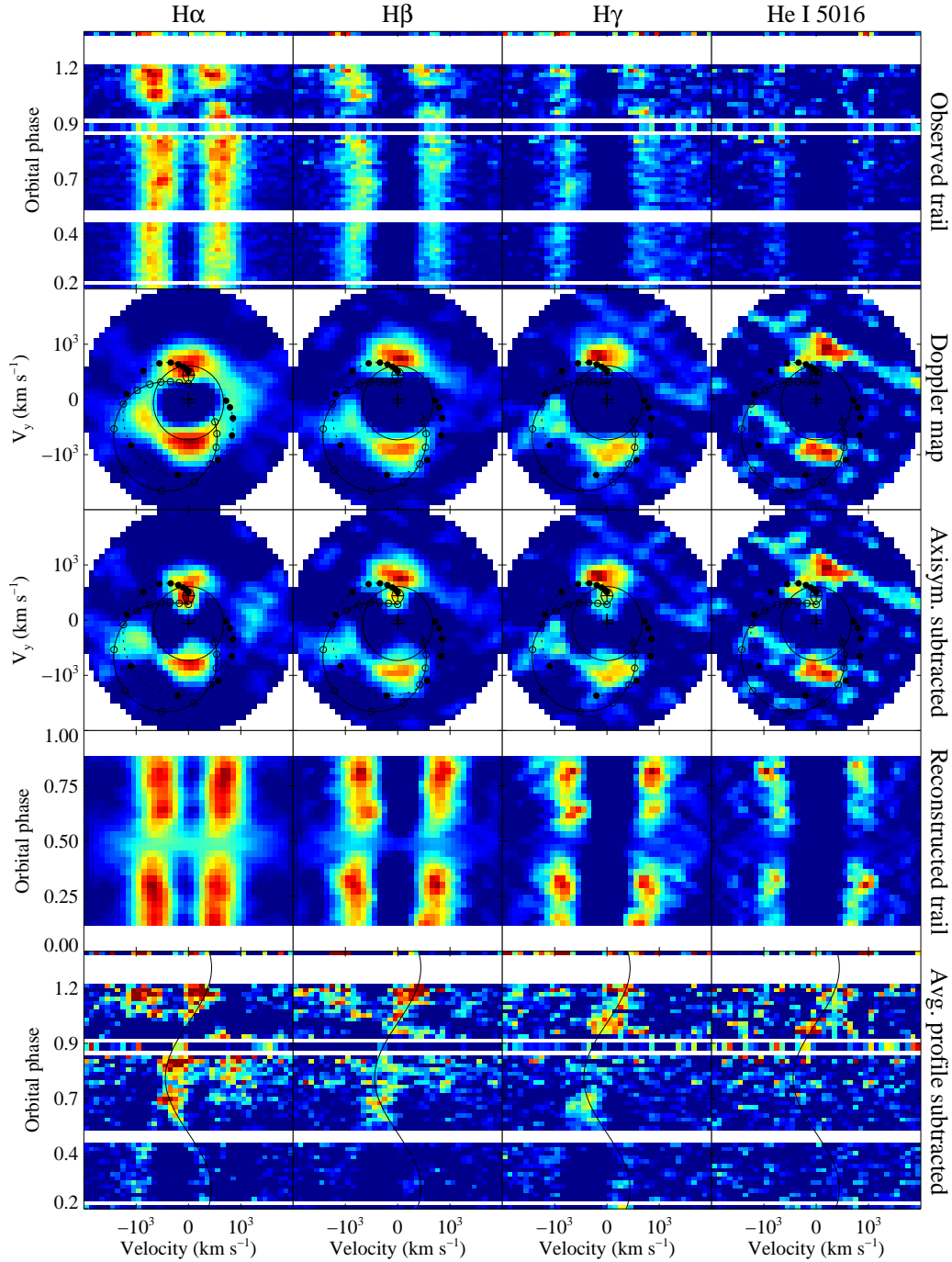


**Figure 10.** Doppler tomography during rise/normal outburst on 6 Jan 2001. *Top, second and fourth row:* As in Fig. 9. *Third row:* Non-axisymmetric component of Doppler maps in second row. *Bottom row:* Observed trail minus average line profile in phase range 0.2 to 0.8, with donor velocity overplotted.

corresponding feature in the trailed spectrogram is brighter when we look at the inner face (phase  $\sim 0.4$ ) than the outer face (phase  $\sim 0.9$ ). Simulations of discs and the stream-disc impact do show vertical structure extended around the disc edge e.g. Armitage & Livio (1996); Hirose, Osaki & Mineshige (1991) and there is much observational evidence for

vertical structure in the outer disc and a flared disc during outburst (e.g. Billington et al. 1996; Ioannou et al. 1999; Naylor et al. 1987). If the core absorption in the lines is due to material in the outer disc along the line of sight to the white dwarf, then the weakening of the core absorption on the Jan 7 points towards changes in the vertical structure

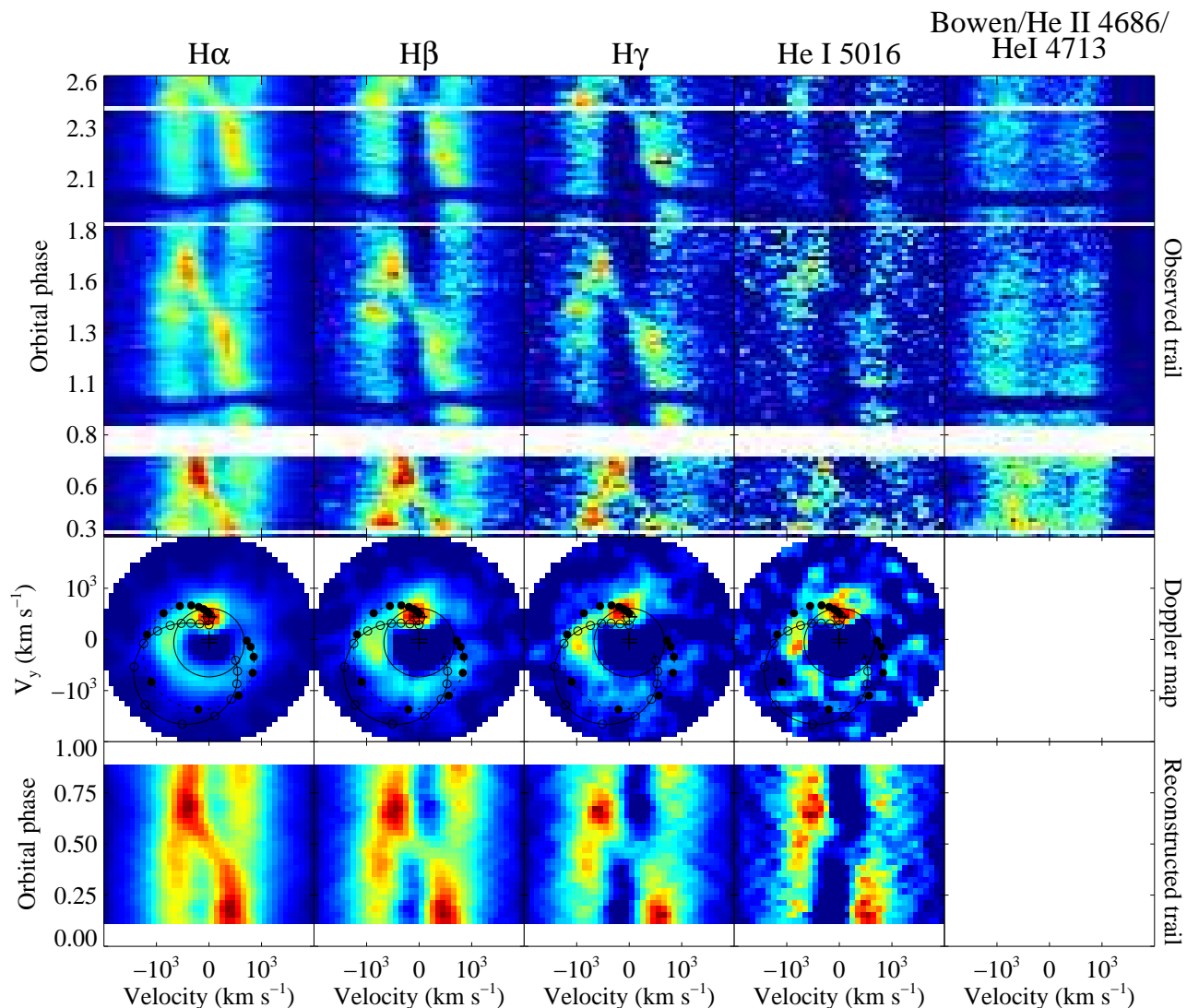


**Figure 11.** Doppler tomography during normal outburst on 7 Jan 2001. Rows as in Fig. 9.

of the outer disc. Such changes might reveal vertical structure around the hotspot on the Jan 7 which was entirely swamped by a uniformly thick outer disc on Jan 6. We expect some reprocessing of the light from the BL throughout the disc, which could explain why the ring extends most, if not all, of the way around the disc in the  $H\alpha$  and  $H\beta$  maps. We conclude that the structure in the Jan 7 maps can be explained by reprocessing of boundary layer EUV and X-ray emission on the inner face of the donor and vertical structure in the disc near to and perhaps triggered by the stream-disc impact.

The reconstructed Balmer and He I trails are consistent with those observed, showing the double peaks, deep core and donor S-wave. The feature around phase 0.4 in the blue wing is smeared out but identifiable.

### 5.3 2000 January: superoutburst

We normalised the line profiles by scaling each so that the integrated line flux above the continuum was the same for all. This reduced the variability in the flux caused by poor observing conditions. These normalised trailed spectra for 2000 Jan 19 (Fig. 12, top row) show the double-peaked structure characteristic of accretion discs. Also present in all lines is the deep core between the disc peaks, which is below the continuum except in  $H\alpha$ . The Balmer lines and He I 6678Å show a narrow partial S-wave that moves from red (phase 1.3) to blue (phase 1.7) and disappears around phase 1.8. This looks like the donor star emission seen during the normal outburst but not during quiescence. We see the inner face of the donor star only during the two bright states, supporting the idea that the donor star is being irradiated. The Doppler maps (middle row of Fig. 12) all show disc emission with asymmetric artefacts like those on 2001 Jan 6,

which resulted from incomplete phase coverage. The donor emission is visible in these maps. The asymmetry probably results from the incomplete phase coverage, though during superoutburst the disc is tidally distorted and precessing, and so asymmetric dissipation patterns and vertical structure in the disc are expected (e.g. Foulkes et al. 2004). The reconstructed Balmer and He I trails show bright red-shifted emission around phase 0.3 and blue-shifted emission around 0.8. This is the donor S-wave crossing the disc peaks, and is not seen in the observed trails because the inner face of the donor will be only half visible at phases 0.25 and 0.75, and is completely invisible around phase 0.

## 6 DISCUSSION

There are several sets of photometry of eclipsing dwarf novae beginning early during the rise to outburst. Vogt (1983) presents the rise to a normal outburst of OY Car, while Webb et al. (1999) presents an entire outburst of IP Peg. Ioannou et al. (1999) presents observations of another short period high-inclination dwarf nova, HT Cas, covering the rise, peak and decline from a normal outburst. Vogt (1983) and Rutten et al. (1992) showed that during the rise to outburst in OY Car, the outer disc rapidly brightens (as it enters the hot ionized state), with this hot bright region quickly propagating inwards towards the white dwarf, the outer radius remaining constant. As the outburst reaches maximum brightness, the radius of the emission region shrinks by about a third. Ioannou et al. (1999) find exactly the same outside-in behaviour in HT Cas, additionally concluding that the disc becomes vertically flared during outburst. In IY UMa the emission region shrinks and the eclipse depth increases between the observed continuum maximum and a day later. This indicates the outer disc returns to quiescence before the inner disc, as the cooling wave propagates inwards. The disc emission region shrinks during decline in most (if not all) dwarf novae, including two dwarf novae where eclipses suggested an outburst beginning in the inner disc and propagating outwards (IP Peg and EX Dra, Webb et al. 1999; Baptista & Catalán 2001, respectively). Eclipse lightcurves at the very start of the outburst are required to distinguish between inside-out and outside-in outbursts from single band photometry alone.

The apparent disappearance of the orbital hump in H $\alpha$  on 4 Jan 2001 immediately preceding the normal outburst while there is still hotspot line emission seen in the Doppler map is curious. It must result from a change in geometry of the hotspot making it equally visible at all phases. This may simply be due to the inherent variability in the stream-disc impact and disc structure, but we note that while the amplitude of the hotspot is variable, none of our other observations show it completely disappearing. The disappearance may be due to a change in the structure of the outer disc as the outburst begins. This would require the outburst to begin in the outer disc, so that there has been no increase in luminosity detected when it occurs.

The delay in the rise of the line emission compared to the rise of the continuum is something which can only be detected in rare (and fortuitous) spectrophotometry in the earliest stages of outburst like those analysed here. The delay is easily understood if the line emission in outburst is

powered by irradiation from the BL and the outburst is of the outside-in type seen in OY Car and HT Cas. The viscous dissipation-powered continuum begins to rise as soon as the outer disc enters the high state, while the emission lines do not become significantly stronger until the heating wave has reached the inner disc the intensity of high energy BL emission and the emission lines it powers. This delay of the lines relative to the continuum is analogous to the UV delay in dwarf nova outburst observations (Wheatley, Mauche & Mattei 2003), where the UV emission (from the inner disc) rises after the visual emission which comes predominantly from the outer disc. The strong He II emission, thought to be powered by irradiation, the Balmer lightcurves mimicking that of He II, the emission from the inner face of the donor star, and the phase-dependent arc of emission in the 2001 Jan 7 lines all support the conclusion that the emission lines are predominantly powered by irradiation during outbursts.

## 7 SUMMARY

Extensive spectroscopic observations of IY UMa have revealed “classic” quiescent accretion flow, with

- strong continuum and line emission from the hotspot region
- a blackbody hotspot temperature of  $\sim 11000$  K
- ionization of hydrogen in the hotspot region suppressing Balmer emission from the disc close to the hotspot.

Rare spectrophotometry of the rise to a normal outburst reveals

- the continuum and line emission regions shrink at the outburst peak
- the rise in emission line flux is delayed relative to the continuum by a few hours to two days
- during outburst Balmer, He II and Bowen blend emission is seen from the disc, while Balmer emission is also seen from the inner face of the donor and possible vertical structure in the outer disc.

We conclude that the 2001 Jan outburst was of the outside-in type, beginning in the outer disc and propagating inwards. Irradiation by EUV and X-rays from the boundary layer powers the emission lines during outburst, with the time taken for mass to move inwards during the outburst explaining the delay between the rise of the continuum and emission line flux.

## 8 ACKNOWLEDGEMENTS

The data presented here have been taken using ALFOSC, which is owned by the Instituto de Astrofísica de Andalucía (IAA) and operated at the Nordic Optical Telescope under agreement between IAA and the NBIfAFG of the Astronomical Observatory of Copenhagen. The Nordic Optical Telescope is operated on the island of La Palma jointly by Denmark, Finland, Iceland, Norway, and Sweden, in the Spanish Observatorio del Roque de los Muchachos of the Instituto de Astrofísica de Canarias. The William Herschel telescope is operated on the island of La Palma by the Isaac Newton Group in the Spanish Observatorio del Roque de

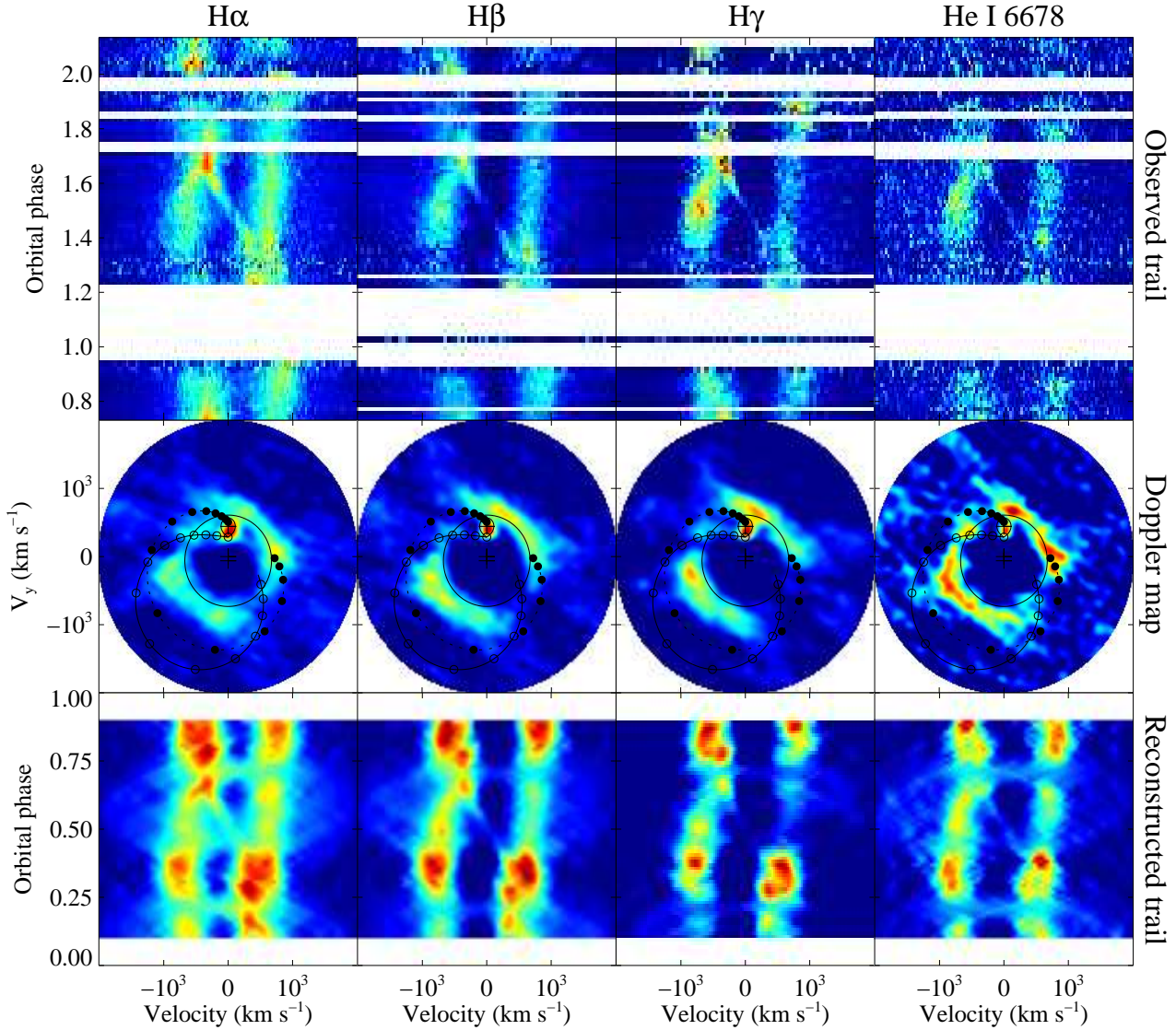


Figure 12. Doppler tomography during superoutburst on 19 Jan 2000. Rows as in Fig. 9.

los Muchachos of the Instituto de Astrofísica de Canarias. DJR was supported by a PPARC studentship and the OU research committee and by a PPARC rolling grant at Leicester. CAH gratefully acknowledges support from the Leverhulme Trust F/00-180/A. LMR was supported by a PPARC post-doctoral grant. The authors gratefully acknowledge the work of the Variable Star Network (VSNET, <http://www.kusastro.kyoto-u.ac.jp/vsnet/index.html>). The reduction and analysis of the WHT data were carried out on the Southampton node of the STARLINK network. The authors thank Rob Hynes for useful comments.

## REFERENCES

- Armitage P. J., Livio M., 1996, *ApJ*, 470, 1024  
 Baptista R., Catalán M. S., 2001, *MNRAS*, 324, 599  
 Billington I., Marsh T. R., Horne K., et al., 1996, *MNRAS*, 279, 1274  
 Deguchi S., 1985, *ApJ*, 291, 492  
 Foulkes S. B., Haswell C. A., Murray J. R., et al., 2004, *MNRAS*, 349, 1179  
 Harlaftis E. T., Marsh T. R., 1996, *MNRAS*, 308, 97  
 Hessman F. V., Koester D., Schoembs R., et al., 1989, *A&A*, 213, 167  
 Hirose M., Osaki Y., Mineshige S., 1991, *PASJ*, 43, 809  
 Honey W. B., Charles P. A., Whitehurst R., et al., 1988, *MNRAS*, 231, 1  
 Ioannou Z., Naylor T., Welsh W. F., et al., 1999, *MNRAS*, 310, 398  
 Marsh T. R., 1989, *PASP*, 101, 1032  
 Marsh T. R., Horne K., 1988, *MNRAS*, 235, 269  
 —, 1990, *ApJ*, 349, 593  
 Marsh T. R., Horne K., Schlegel E. M., et al., 1990, *ApJ*, 364, 637  
 Marsh T. R., Horne K., Shipman H. L., 1987, *MNRAS*, 225, 551  
 Morales-Rueda L., Marsh T. R., 2002, *MNRAS*, 332, 814  
 Morales-Rueda L., Marsh T. R., Billington I., 2000, *MNRAS*, 313, 454  
 Naylor T., Charles P., Hassal B., et al., 1987, *MNRAS*, 229, 183  
 Osaki Y., 1996, *PASJ*, 108, 39  
 Osaki Y., Meyer F., 2003, *A&A*, 401, 325



- Patterson J., Augusteijn T., Harvey D. A., et al., 1996, *PASP*, 108, 748
- Patterson J., Kemp J., Jensen L., et al., 2000, *PASP*, 112, 1567
- Patterson J., Raymond J. C., 1985, *ApJ*, 292, 550
- Robinson E. L., Nather R. E., Patterson J., 1978, *ApJ*, 219, 168
- Robinson E. L., Wood J. H., Bless R. C., et al., 1995, *ApJ*, 443, 295
- Rolfe D. J., 2001, PhD thesis, The Open University
- Rolfe D. J., Abbott T. M. C., Haswell C. A., 2001a, in *Proc. Astro-Tomography Workshop*, Boffin H., Steeghs D., eds., Springer-Verlag Lecture Notes in Physics
- , 2002a, in *Proc. The Physics of Cataclysmic Variables and Related Objects*, Gänsicke B. Beuermann K. R. K., ed., ASP conference series
- , 2002b, *MNRAS*, 334, 699
- Rolfe D. J., Haswell C. A., Patterson J., 2001b, *MNRAS*, 324, 529
- Rutten R. G. M., Dhillon V. S., Horne K., et al., 1993, *Nature*, 362, 518
- Rutten R. G. M., Kuulkers E., Vogt N., et al., 1992, *A&A*, 265, 159
- Spruit H. C., Rutten R. G. M., 1998, *MNRAS*, 299, 768
- Stanishev V., Kraicheva Z., Boffin H. M. J., et al., 2001, *A&A*, 367, 273
- Steeghs D., 2001, in *Proc. Astro-Tomography Workshop*, Boffin H., Steeghs D., eds., Springer-Verlag Lecture Notes in Physics
- Steeghs D., Perryman M. A. C., Reynolds A., et al., 2003, *MNRAS*, 339, 810
- Tuohy I., Remillard R., Brissenden R., et al., 1990, *ApJ*, 359, 204
- Vogt N., 1983, *A&A*, 128, 29
- Webb N. A., Naylor T., Ioannou Z., et al., 1999, *MNRAS*, 310, 407
- Wheatley P., Mauche C., Mattei J., 2003, *MNRAS*, 345, 49
- Wood J. H., Horne K., Berriman G., et al., 1986, *MNRAS*, 219, 629
- Wu X., Li Z., Gao W., et al., 2001, *ApJ*, 549, L84